ALMA MATER STUDIORUM – UNIVERSITÀ DI BOLOGNA

CAMPUS DI CESENA

DIPARTIMENTO DI

INGEGNERIA DELL'ENERGIA ELETTRICA E DELL'INFORMAZIONE

"GUGLIELMO MARCONI"

CORSO DI LAUREA IN INGEGNERIA BIOMEDICA

TITOLO DELL'ELABORATO

CHARACTERIZATION OF BLASTIC BONE TISSUE THROUGH NANOINDENTATION TEST

Elaborato in

Comportamento Meccanico Dei Biomateriali E Delle Strutture (c.i.)

Relatore

Prof. Joseph Lovecchio

Presentata da

Alessandra Di Lorenzo

Correlatori

Dr. Marco Palanca

Dr. Enrico Dall'Ara

Dr.ssa Giulia Cavazzoni

Anno Accademico 2021/2022

Abstract

La colonna vertebrale è comunemente affetta da metastasi, che possono alterare le normali proprietà meccaniche dell'osso. Indagare gli effetti delle metastasi a livello nanostrutturale e comprendere la relazione tra quantità dell'osso, qualità dell'osso e proprietà meccaniche può migliorare la previsione della comparsa di fratture dovute alle metastasi.

Lo scopo di questo lavoro è stato quello di valutare le proprietà meccaniche, come durezza, modulo elastico, lavoro totale, lavoro elastico e lavoro dissipato del tessuto blastico.

In questo lavoro, tredici provini dal nucleo di vertebre lombari affette da metastasi blastiche sono stati preparati e sono state effettuate nanoindentazioni su differenti gruppi di provini (tessuto trabecolare lamellare, tessuto blastico lamellare, tessuto blastico non organizzato) per indagare le potenziali differenze tra quelli con un'apparenza sana e quelli con un'apparenza metastatica.

I risultati ottenuti dall'analisi statistica hanno mostrato che durezza e modulo elastico risultavano inferiori (4.1% e 3.5% rispettivamente) nei provini blastici non organizzati quando questi sono stati messi a confronto con provini lamellari. Similarmente, la durezza è risultata inferiore (4.1%) nei provini blastici non organizzati quando questi sono stati messi a confronto con quelli blastici lamellari. Inoltre, mediante un'analisi di correlazione, è stata trovata una relazione significativa tra il modulo elastico e la durezza nel caso dei provini blastici lamellari e blastici non organizzati. Infine, il lavoro totale è risultato maggiore (2.8%) nei provini blastici non organizzati quando questi sono stati messi a confronto con quelli trabecolari lamellari.

In conclusione, i risultati di questo studio evidenziano l'importanza di indagare le proprietà meccaniche locali del tessuto blastico per valutare la competenza meccanica delle vertebre metastatiche a livello nanostrutturale.

Parole chiave: metastasi blastiche; proprietà meccaniche; nanoindentazione.

Abstract

The spine is commonly affected by metastases, which may alter the normal mechanical properties of the bone. Investigating the effects of metastases at the nanostructural level and understanding the relationship between bone quantity, quality, and mechanical properties can improve the prediction of fracture occurrences due to metastases.

The aim of this study was to evaluate the mechanical properties, such as hardness, elastic modulus, total work, elastic work and dissipated work of the blastic tissue.

In this work, thirteen bone cores were prepared from lumbar vertebrae affected by blastic metastases and nanoindentations were performed on different groups of specimens (i.e. trabecular lamellar tissue, blastic lamellar tissue, blastic non organized bone tissue) in order to investigate potential differences between those with a healthy appearance and those with a metastatic appearance. The results obtained from the statistical analysis showed that hardness and elastic modulus were lower (4.1% and 3.5% respectively) in blastic non organized bone specimens when they were compared to lamellar specimens. Similarly, hardness resulted to be lower (4.1%) in blastic non organized specimens when they were compared to blastic lamellar specimens. Moreover, through a correlation analysis, a significant relationship was found between elastic modulus and hardness in the case of blastic lamellar and blastic non organized bone specimens. Finally, the total work resulted to be higher (2.8%) in blastic non organized bone specimens when they were compared to trabecular lamellar specimens.

In conclusion, the outcomes of this study highlight the importance of investigating the local mechanical properties of blastic tissue to assess the mechanical competence of metastatic vertebrae at the nanostructural level.

Key words: blastic metastases; mechanical properties; nanoindentation.

Contents

1. Introduction

1.1 Motivations

1.1.1 Bone Metastasis

Metastases are secondary tumours, which occur when cancer cells move from their original site, where the primary tumor is located, to another organ. Due to the improvements of the therapies, long life expectancy of patients with tumors has increased and consequently the number of patients who are diagnosed metastatic cancer is increasing.

Bone is one of the favourites sites in which metastases spread because of several factors, such as the high blood flow in the area of red marrow. Furthermore, the tumor cells produce adhesive molecules that bind them to marrow stromal cells and bone matrix.

According to the “seed and soil hypothesis”, the combination of these mechanisms provide a fertile ground in which tumor cells can grow.

The presence of the metastases impacts bone remodelling inducing three possibly scenarios based on the radiological appearance: *osteolytic* (Fig. 1), when the process of bone resorption by the osteoclasts exceeds the activity of the osteoblasts, resulting in bone degradation; *osteoblastic* (Fig. 2), when cancer cells release substances to stimulate the osteoblast lineage to increase osteoblast differentiation and new bone deposition [23]. The third possibility is the presence of both (*mixed*).

Osteoblastic metastases induce alterations of the regular process of bone homeostasis that is the process of bone resorption by osteoclasts, followed by the deposition of new bone tissue by the osteoblasts. Indeed, osteoblastic metastases in bone tissue affect the regular bone homeostasis and consequently, the osteoblasts activity exceeds the bone resorption by the osteoclasts. In addition, the cancer cells induce osteoblasts activity and consequently osteoblasts release grow factors, which facilitate tumor growth, inducing a vicious circle [23].

Due to the altered balance of the bone remodelling process, in patients with blastic lesions the degree of mineralization, that is the mineral density at the level of calcified bone tissue, is lower than comparable sites in patients without metastases [2]. Moreover, human vertebral bone with blastic lesion exhibits higher bone volume to trabecular volume fraction and higher trabecular number compared to normal bone [26]. Furthermore, trabeculae affected by osteoblastic metastases are shorter and thicker for a given bone volume to trabecular volume fraction than trabeculae in osteolytic bone [2]. In addition, they present a lower degree of structural anisotropy [26].

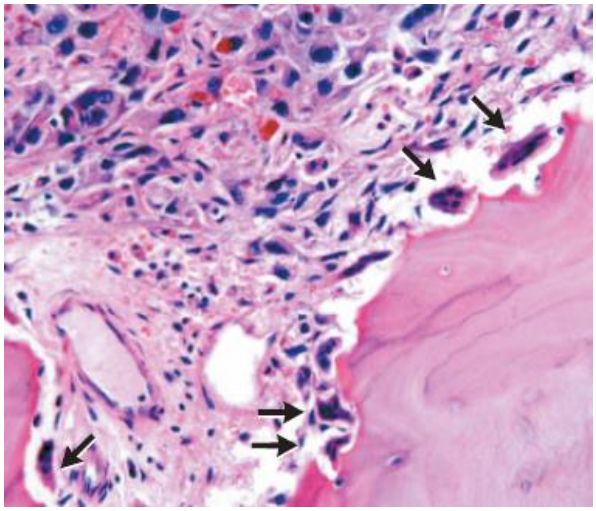

Fig.1: Osteolytic bone metastasis (hematoxylin and eosin, x200); osteoclasts (arrows) [23].

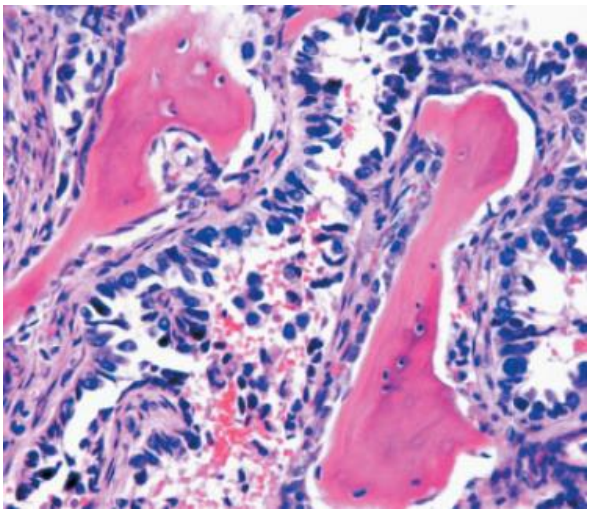

Fig.2: Osteoblastic metastasis (hematoxylin and eosin, x200) [23].

1.1.2 Clinical management

The column spine is the most common site of osseous metastases involving approximately 40% of patients [28]. Primary tumors that most often lead to bone metastasis are prostate, breast, kidney, lung, and thyroid cancer [21] and about 60-70% of patients with systemic cancer will have spinal metastases [25].

Spine metastases are associated with skeletal-related events such as pathological fractures and spinal cord compression, which diminish patient's life quality and impact survival [24]. Currently, the therapeutic options to manage vertebral metastases include radiation therapy, systemic therapies and surgery and they aim to achieve pain palliation and local tumor control [27].

The altered distribution of the bone tissue inside the metastastic vertebra can often cause mechanical instability of the spine [3]. The Spine Oncology Study Group (SOSG) defines spine instability as loss of spinal integrity as a result of a neoplastic process that is associated with movement-related pain, symptomatic or progressive deformity, and/or neural compromise under physiologic loads [7]. Surgical treatment decisions are based on spinal stability and patient-specific factors that include patient health, prognosis, and tumor histology [7].

Due to the complexity of the pathological condition, the cooperation of many experts, such as oncologists, radiologists and orthopaedic and/or neurosurgical spine surgeons, is needed. Prompt treatment has been shown to play a crucial role in improvement of the quality and duration of remaining life [17].

In order to facilitate the comprehension among different operators, the multidisciplinary spine team at Memorial Sloan-Kettering Cancer Center (MSKCC) has developed and used a decision framework for metastatic spine disease, NOMS, which incorporates four fundamental assessments: neurologic, oncologic, mechanical instability, and systemic disease [16]. The purpose of the NOMS is to provide the framework to assess the most appropriate treatment of spinal metastases, among the use of radiation, surgery or systemic therapy for the individual patient [16].

In NOMS, mechanical instability is a separate consideration defined for pathologic fractures [16]. Although radiotherapy has effects on local tumor control, it has no effect on spinal stability. Spinal surgery is a high risky treatment that could aggravate the conditions of the patients, leading to a reduction of the quality of life. Thus, assessment of mechanical stability is a crucial indicator for the surgical decision-making process, regardless of the neurologic or oncologic assessment.

The Spinal Instability Neoplastic Score (SINS) is a scoring system, which has the purpose of evaluating the degree of spinal instability and facilitating appropriate referrals among spine oncology specialists. SINS categorizes risk of spinal instability assessing and scoring 6 parameters: vertebral level, mechanical pain, bone lesion quality, radiographic alignment, vertebral body collapse and posterolateral spinal element involvement (TABLE 1).

The summed score results to be ranging from 0 to 18 points [28], based on one clinical parameter and five radiographic parameters and, in accordance to the points given, mechanical instability is assessed: stable (0-6 points), impending/potentially instable (7-12 points) and unstable (13-18 points). In most of the cases, metastases result to be impending/potentially instable (TABLE 2).

Table1: Summary Table Including All Elements of the SINS [7].

	Score
Location	
Junctional (occiput-C2, C7-T2, T11-L1, L5-S1)	3
Mobile spine (C3-C6, L2-L4)	2
Semirigid (T3-T10)	1
Rigid (S2-S5)	0
Pain	
Yes	3
Occasional pain but not mechanical	1
Pain-free lesion	0
Bone lesion	
Lytic	2
Mixed (lytic/blastic)	1
Blastic	0
Radiographic spinal alignment	
Subluxation/translation present	4
De novo deformity (kyphosis/scoliosis)	2
Normal alignment	0
Vertebral body collapse	
>50% collapse	3
<50% collapse	2
No collapse with >50% body involved	1
None of the above	0
Posterolateral involvement of spinal elements	
Bilateral	3
Unilateral	1
None of the above	0
Total score	
Stable	0–6
Indeterminate	7–12
Unstable	13–18

Table 2: SINS scores organized as a total score, three-clinical categories, and binary scale with their corresponding levels of stability where surgical consultation is recommended for a total score ≥ 7 [8].

Total Score (0-18 SINS)	1	2	3	4	5	6	7	8	9	10	11	12	13	14	15	16	17	18
Three Clinical Categories (3-point)			Stability					Potentially Unstable							Unstable			
Binary Scale (2-point)			Stability					Current or potential instability; Surgical consultation recommended										

It has been demonstrated that after the introduction of the SINS in the clinical practice, there was an important decrease in both the median and the mean assessed overall score in both radiotherapy and

surgical patients. This can be explained by increased awareness of spinal neoplastic related instability and more appropriate referral of patients to spinal surgeons after the introduction of the SINS [7].

However, scoring systems used to assess spinal stability lack specificity [18] and in many cases they do not provide clear guidelines [4]. Moreover, it has been shown that SINS fails to identify true negative cases (specificity equal to 79.5%) [8].

According to Fisher et al. [9], SINS requires prospective clinical validation, since in 20% of the cases were considered stable by surgeons, while they were classified as potentially unstable by the radiologists. Furthermore, when metastases result to be impending/potentially instable there is a lack of clear guidelines and consequently, treatment decisions are taken according to the experience of the clinicians. In addition, no significant correlations were found between the SINS values and the mechanical properties of vertebrae [4].

1.1.3 Preliminary biomechanical evidence

However, it has been shown that the presence of metastatic lesions affects the bone quantity, architecture and bone quality [2]. Since bone structure, architecture, and material composition are significant contributors to fracture resistance, the presence of metastatic lesions affects the distribution of loads and strains in the metastatic bone.

Biomechanical evidence of the metastasis effect were widely explored through experimental and computational methods to help the prediction of vertebral fracture. However, only the overall mechanical properties are usually investigated. This approach partially explain the complexity of the problem and the local consequences of metastatic disease may be hidden [18].

Limited studies have investigated the local effects induced by osteoblastic metastases on the mechanical competence of human vertebrae. Stadelmann et al. [26] evaluated the impact of tumor-induced bone metastases on the structure tissue-level, and organ-level mechanical properties of human vertebral bone. However, they provided limited description of the mechanical behaviour of the singular lamella.

Investigating the effects of metastases at the nanostructural level and understanding of the relationship between bone quantity, quality, and mechanical properties can improve the prediction of fracture occurrences due to metastases reducing the associated morbidity.

1.2 Bone properties

The mechanical strength of the bone is influenced by its apparent density (the mass of bone present in the volume of interest), architecture (the geometric distribution of the mass) and the intrinsic bone material properties (bone matrix and mineral composition) [2].
Bone quality includes all the factors that contribute to bone fracture independently of bone mineral density.

Mechanical bone quality depends on many parameters, including:

1. stiffness, intended as the ability to resist elastic/reversible deformation;
2. strength, that is the ability to resist plastic/permanent deformation;
3. toughness, the ability to absorb energy during deformation;
4. fracture toughness, the ability to prevent cracks from initiating and progressing.

Due to the hierarchical structure of the bone, the evaluation of the properties at different length scales (Fig.3) can assess the bone quality. The factors that contribute to bone quality are [10]:

1. whole bone morphology, defined by the amount and distribution of bone tissue;
2. the overall composition of bone tissue, depending on the proportion of hydroxyapatite, water, type I collagen, and other non-collagenous proteins;
3. the biophysical properties of these components, such as the degree and type of collagen cross-linking and the mineral crystal size and their crystallinity.

The two principal constituents of the bone matrix are the hydroxyapatite and the type-I collagen, where the crystals of hydroxyapatite are collocated. These components affect the bone quality not only at a nano-level but also across many length scales.

The extracellular matrix (ECM) characteristics depend on its composition and organization, which are affected by proteins and signalling pathways. These characteristics in turn affect the bone ECM material properties, such as elastic modulus and hardness.
In particular, the ECM elastic modulus is affected by the mineral concentration, whereas type-I collagen content and maturity of collagen crosslinking affect the bone toughness and post-yield deformation [2].

Moreover, hydroxyapatite mineral is associated with bone material stiffness, while collagen mutations can deregulate the coupled remodelling of bone by osteoblasts and osteoclasts, the maintenance of bone mass, and the organization of mineralized collagen fibrils.
In addition, defects in the lamellar structure limit the ability to prevent growth crack [1].

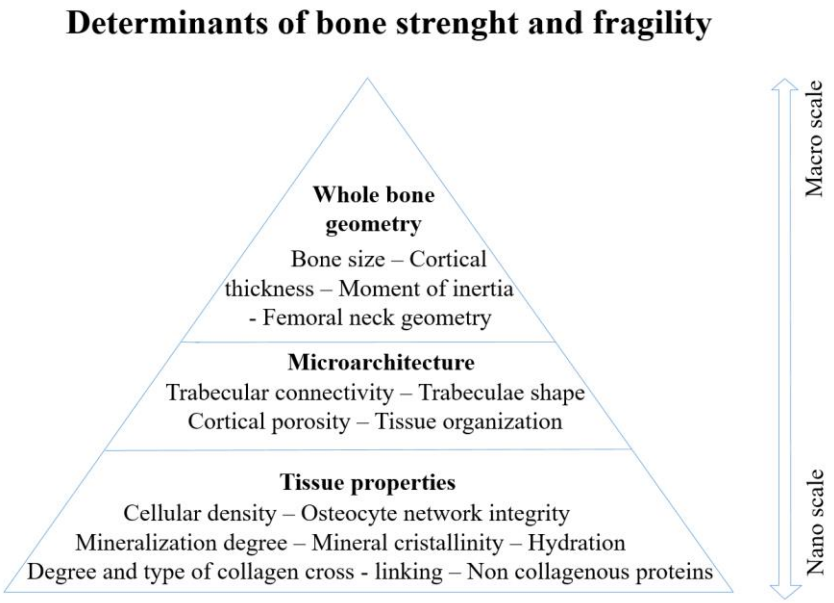

Figure 3: The several traits influencing bone strength are schematically depicted in the the figure (adapted from [10]).

The ECM properties are also sensitive to pathways that regulate bone remodelling by osteoblasts, osteoclasts, and osteocytes [1]. Moreover, non-collagenous proteins have been shown to play a structural role in bone facilitating microdamage formation and energy dissipation [2].

1.3 Investigation methods

In order to study the properties at the specific levels of organization, different techniques must be implemented for the characterization of the features of the bone (Fig.4).

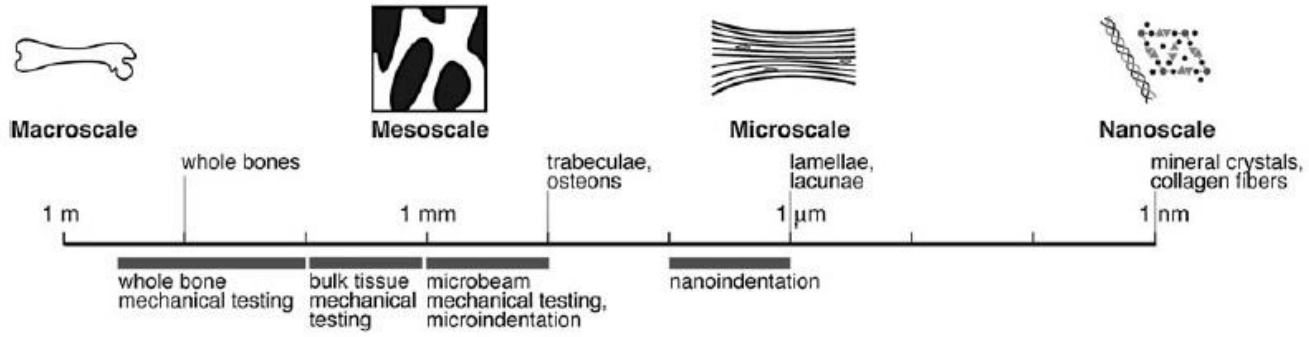

Figure 4: The hierarchical structure of bone is depicted schematically on a logarithmic scale. Techniques for mechanical (dark gray bars) [6].

Current methods to study the bone at a nanostructural level are nano-computed tomography (nano-CT) and nanoindentation.

Nano-computed tomography is a high resolution CT-technology for 3D imaging at sub-micrometer resolution [14]. The micro-CT imaging make it possible to investigate the composition and the structural properties of mineralized tissue at a quantitative three-dimensional level. Consequently, this imaging technique facilitates non-destructive, rapid, 3D quantification of morphology and density, which are indicators of the tissue and organ-level homeostasis [15].

However, due to the resolving capabilities of micro-CT systems, the characterization of small structures such as microstructural components of bone and individual cells is not possible. The introduction of nano-CT technology during the past decades opened the door to imaging small structures, even down to the cellular scale, with markedly improved contrast [15]. By improvement of the spatial resolution, structures at a cellular level, such as osteocyte lacunae, become visible [14]. The choice of spatial resolution is crucial to obtain a satisfactory image of a given structure. The trabecular bone is generally investigated with a voxel size between 5 μm and 20 μm. To enable the imaging of lacunae and canaliculi, a spatial resolution at the micrometer or nanometer scale is required [20]. The nano-CT technology has enabled ultra-high resolution imaging by utilizing a powerful nano-focused X-ray source [15]. These machines generally use a nano focal spot source (<400 nm) [20]. Nano-CT allows the assessment of bone tissue properties on the lamellar scale, including nanoporosity, quantification of mineralization and collagen fibers [20].

One of the limitations of the X-ray nano-CT is that this technique could be related to the long image acquisition times [20], thus the imaging may be affected by the viscoelastic properties of the bone tissue. Moreover, large amounts of data storage space are needed, even for a single study [15].

Surface and interfacial properties are very important in biology and biomaterials, hence there is a growing interest in the use of nanoindentation technique to investigate biological surfaces and materials. Indentation consists in pressing a hard tip (indenter) with a well-defined geometry and with a known force into a semi-infinite half-space and measuring directly or indirectly the contact area (Fig.5) [19]. During the test, the applied load and the depth of penetration are continuously monitored. The area is measured optically after the removal of the indenter and from the resulting load-depth trace and probe area function, the mechanical properties are calculated [13].

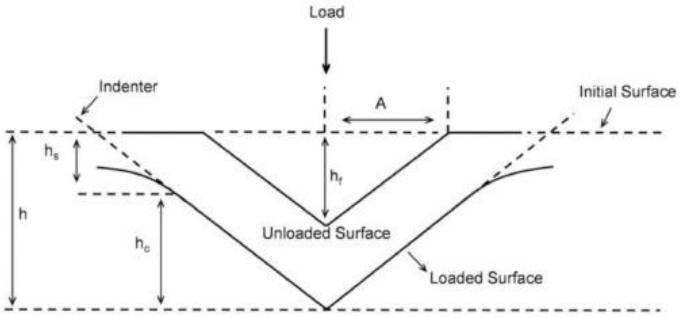

Figure 5: Schematic representation of the contact geometry during loading and unloading of the indenter tip and parameters used to obtain the hardness and Young's modulus of the material. h: total depth during loading; A initial projected contact area; hf: final depth after sample deformation; hc: contact depth; hs: displacement of the perimeter next to tip-contact region [11].

Nanoindentation presents many advantages: it allows determining many properties of the materials, such as elastic modulus, hardness values, creep, yield stress, work and compliance. Furthermore, it is possible to determine dynamic characteristics such as dynamic elastic modulus, load-induced phase transition, strain rate sensitivity. Another advantage of nanoindentation is its ability to probe small volumes of materials. Since smaller loads have been used to investigate small samples, thin films or to measure local hardness, the extent of the residual indentations was reduced so that it could no longer be measured with sufficient accuracy by a simple optical method. Hence, this technique allows the characterization of the nano- scale bone structure, up to lamellar regions.

The isotropic and anisotropic indentation analyses can be used for moderately rate-dependent (viscoelastic and/or viscoplastic) materials such as bone [19]. Therefore, during the nanoindentation test a loading ramp with a constant load rate is applied and then it is hold for a specific period of time (typically from 5 to 120 s) with a constant load, and then it is followed by an unloading ramp (Fig.6) [29].

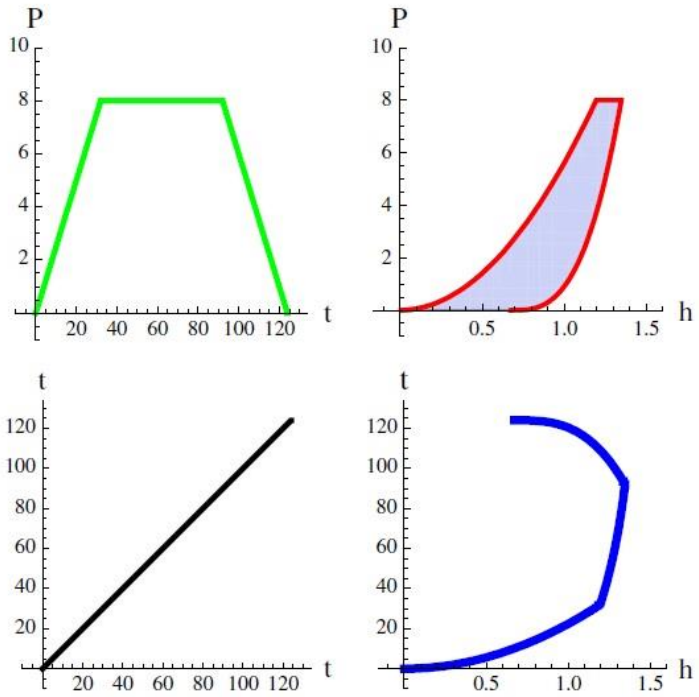

Figure 6: A typical load controlled indentation schedule with the resulting displacement of the tip [29].

Since nanoindentation is a depth-sensing technology, the accuracy of the instrument adopted can be affected by many factors, including a dirty or damaged probe, calibration material surface properties, operator bias, errors in data fitting and the limitation of the spatial resolution due to the specimen surface roughness [13].

In *Mechanical properties of human trabecular bone lamellae quantified by nanoindentation* a heterogeneity in mechanical properties has been found among the bone lamellae and individuals, and this factor is crucial to understand bone integrity [30].

Critical assumptions of this technique are [31]:

• The constitutive behaviour of the specimen is elastic with time-independent plasticity;

• The solution for the elastic deformation of an irreversibly indented surface geometry is like the one of a flat semi-infinite half space;

• The Poisson ratio ν of the specimen is known.

In order to perform micro- or nano- indentations, indenters with a well-defined tip geometry and material are used; the Berkovich probe is the standard probe used to perform nanoindentations [12] and it was used also in this study.

The theoretical basis of the method relies on the Boussinesq solution of indentation of an elastic half-space by a rigid, axisymmetric indenter derived by Sneddon [19]. The relationship between contact stiffness and the elastic properties of the sample is the following [31]:

$$\frac{dP}{dh} = \frac{2}{\sqrt{\pi}}\sqrt{A}\frac{E_s}{(1-{\nu_s}^2)}$$

where P is the load, h is the penetration depth, A is the projected contact area of the indenter as a function of depth h, E_b is the elastic modulus and ν_b is the Poisson ratio of the specimen.

Application of this solution to the unloading procedure of nanoindentation with a deformable pyramidal Berkovich tip was then proposed by Oliver and Pharr. The relationship between contact stiffness and the elastic properties of the sample becomes [31]:

$$\frac{dP}{dh} = \beta\frac{2}{\sqrt{\pi}}\sqrt{A}E_r$$

where b is an empirical indenter shape factor and the reduced modulus E_r is given by [31]:

$$\frac{1}{E_r} = \frac{(1-{\nu_s}^2)}{E_s} + \frac{(1-{\nu_i}^2)}{E_{ind}}$$

with the indices ind and s corresponding to the indenter and the sample, respectively.

Hardness (H), which is one of the parameters calculated during the study, is defined by an applied force (P) divided by area [29]:

$$H = \frac{P}{A}$$

where A is either the residual area A_r of the imprint or the estimated contact area A_c using deep-sensing instruments. During an indentation test, the change in loading rate, the penetration velocity of the tip and consequently the strain rate, results in a change in the calculated hardness.

Regarding analysis of a typical force-displacement indentation curve (Fig. 8), a reduced modulus (Er) can be related to the slope of the unloading curve at the maximum load [29]:

$$\frac{1}{E_r} = \frac{\sqrt{\pi}}{2\beta\sqrt{A_c}}\frac{dP}{dh}(h_{max}) = \frac{1-{\nu_{ind}}^2}{E_{ind}} + \frac{1-{\nu_t}^2}{E_t}$$

where A_c is the contact area, β is a tip shape factor, E_t and ν_t are elastic modulus and Poisson's ratio of the tip, and E_{ind} and ν_{ind} are the indentation modulus and Poisson's ratio of the tested material. This relationship assumes absence of friction between the indenter and the material.

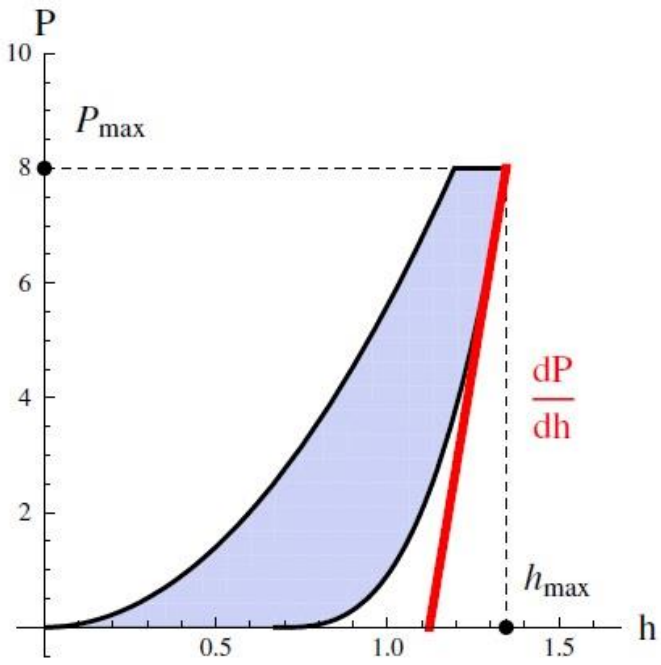

Figure 8: Indentation curve with the unloading stiffness and the dissipated work [29].

An indicator investigated during the project was the elastic modulus. Bone tissue is usually considered as isotropic and homogeneous. For isotropic materials, the relationship between the indentation modulus of rateindependent (nonviscous) materials, the elastic modulus E and Poisson's ratio ν, the following [29]:

$$\frac{1}{E_{ind}} = \frac{1-\nu^2}{E}$$

Another important parameter investigated during the study was the work. In particular, there are three work definitions:

- Indentation work (W)
- Elastic work (W_e)
- Dissipated work (W_d)

The indentation work is determined numerically from the force-displacement curves, using the trapezoidal rule. In order to obtain the elastic work, an integration is executed along the loading part up to the end of the hold time. Dissipated work is obtained subtracting the W_e from the W.

1.4 Aim

Due to the presence of osteoblastic metastases, the organization of the blastic tissue is different from the organization of the trabecular tissue. Indeed, the latter appears highly organized, while the former does not have a defined organization and the tissue presents a lower degree of structural anisotropy.

Consequently, the initial hypothesis is that the blastic tissue and the trabecular tissue present different mechanical properties.

The aim of the study is to examine specimens of human vertebrae affected by blastic metastases, using the nanoindentation technique, in order to test the previous hypothesis. This is made possible through the investigation of the following parameters:

- Hardness
- Elastic modulus
- Total work

- Elastic work
- Dissipated work

2. Materials and methods

2.1 Specimens collection

In this project both the ethics committees of the University of Bologna (n. 17325, 08/02/2019) and the University of Sheffield (n. 031782, 22/06/2020) approved all the procedures. Human spines with vertebrae affected by blastic metastases were obtained through an ethically approved international donation program (Anatomy Gift Registry, USA).

The details of the donors in terms of kind of primary tumour, age, race, genre, height, and weight are reported in the Table 3.

Table 3: Donors details.

Specimen	Cancer	Age	Race	Sex	Height (cm)	Weight (kg)	BMI
#777_L4	Prostate	78	C	M	183	54	16
#773_L2	Prostate	66	C	M	175	66	21
#773_L4	Prostate	66	C	M	175	66	21
#766_L1	Adrenal	81	C	M	183	77	23

2.2 Specimens preparation

The preparation of the specimens refers to the protocol developed by the University of Sheffield in order to perform the nanoindentation tests.

2.2.1 Bone cores preparation

All the soft tissues around the vertebra were removed except for the intervertebral discs. The endplate was removed using a diamond band saw and then a first slice of 3 mm height was cut. Afterwards, a second slice of 4 mm height was cut (Fig.9). The cuts were performed using the Exakt bandsaw (300/30 model) with a diamond blade (Figure 10). The obtained specimen was then cleaned with a water-jet.

The bone cores were prepared from the 4 mm slices using a driller and diamond core bits with a diameter of 3 mm. For each slice, 4 cores were extracted (Fig.11).

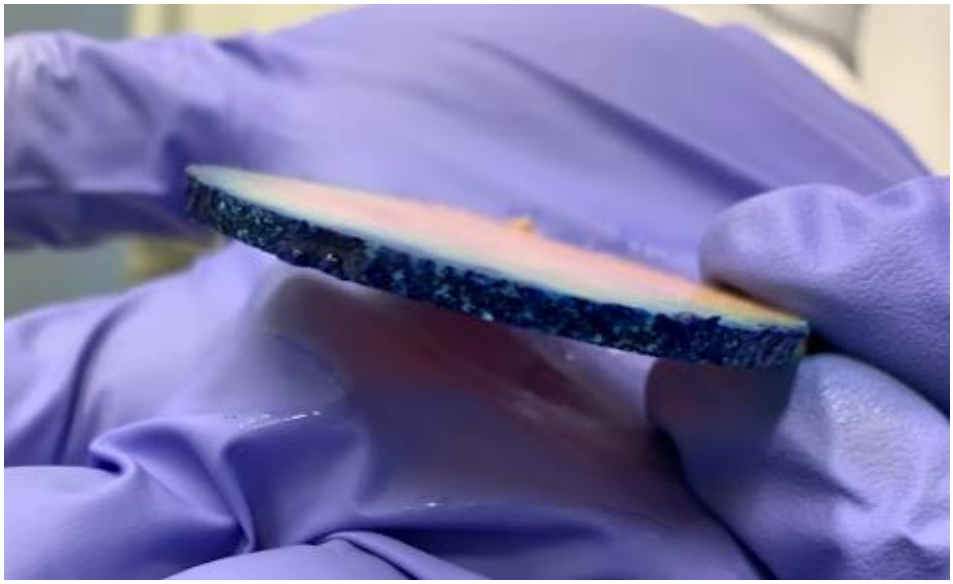

Figure 9: 4 mm slice from metastatic vertebra cut using the Exakt bandsaw (300/30 model).

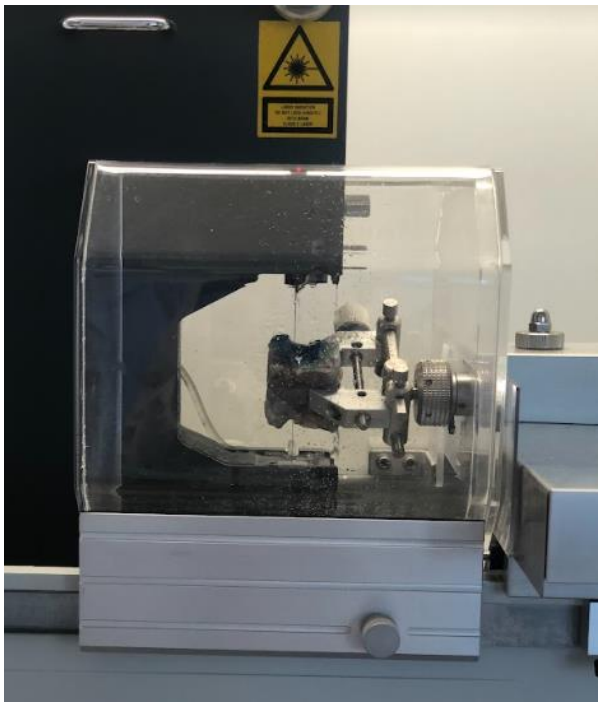

Figure 10: Exakt bandsaw (300/30 model) with diamond blade.

The first core was obtained from the central portion of the slice, the second core was obtained from the anterior portion of the slice, while the last two cores were performed in the medial ad lateral

position with respect to the lesion. Then an only blastic core and a core from only healthy trabecular bone were obtained.

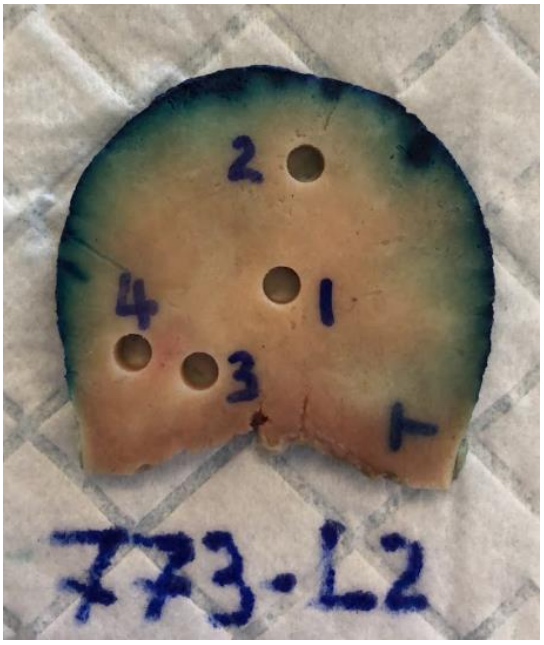

Figure 11: bone cores obtained from the donor #773, vertebra L2.

Afterwards bone marrow and the soft tissues were removed from the bone cores firstly using warm water and hand soap, then water jet and pliers and, if necessary, ultrasound bath.

The specimens were left 5/6 hours (overnight) in order to let them dry. Thereafter, the specimens were put in caps with a diameter of 6 mm.

2.2.2 Embedding

The embedding procedure consists in including the specimen with epoxy resin to support the bone tissue during the nanoindentation tests.

The epoxy resin was obtained preparing a solution composed by 10 mL of epofix resin mixed with 1.3 mL of epofix hardener. Afterwards the caps were filled with the prepared epoxy resin and then they were put in a vacuum chamber. The specimens were placed in a vacuum chamber to remove the bubbles from the internal portion of the specimen.

The vacuum was prepared connecting the vacuum chamber with the pipe to the tap on the desk. In order to make the vacuum, the valve was opened. Once the vacuum was obtained, the valve gas was closed and the specimens were left there for 10 minutes. Afterwards, the vacuum valve was opened paying attention to not including airs and to not making the specimens jump out. Then, the vacuum chamber was opened and the specimens. The bone cores were realigned in the case they tilted in the tubes. Then the resin was left hardening for the following 12 hours (Fig.12).

Figure 12: bone specimen embedded in epoxy resin.

2.2.3 Polishing

The specimens were polished in order to reduce the surface roughness before they were tested through nanoindentation.

Sand papers with different roughness were used to expose the bone and to make the two surfaces of the specimens parallel. Three types of sand papers were used to perform the polishing procedure, in the following order: P400, P800, P1200. The following step consisted in the polishing by using alumina 0.05 μm size particles.

The procedure was applied for each specimen.

Between each step of polishing the microscope Olympus CH-2 with a 50x magnification was used to observe the structure of the bone in each specimen and to save the obtained images.

2.3 Nanoindentation tests

During the nanoindentation tests, three types of bone tissue were investigated according to the microscope appearance of the specimens: the trabecular lamellar tissue (Fig.13), the blastic lamellar tissue (Fig.14) and the blastic non organized tissue (Fig.15).

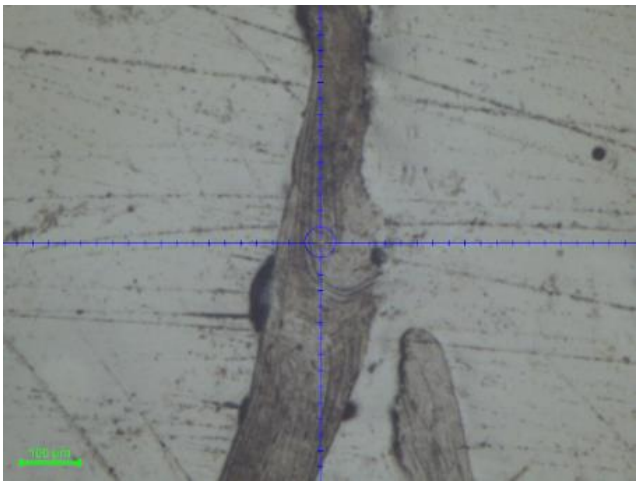

Figure 13: Light microscope image from trabecular lamellar tissue, Olympus CH-2, scale bar 100μm.

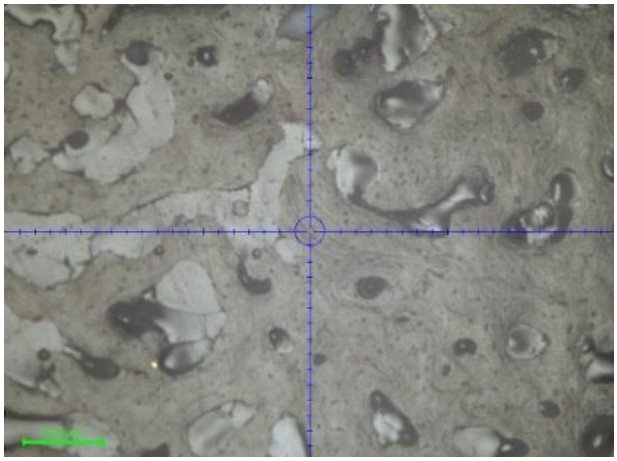

Figure 14: Light microscope image from blastic lamellar tissue, Olympus CH-2, scale bar 200μm.

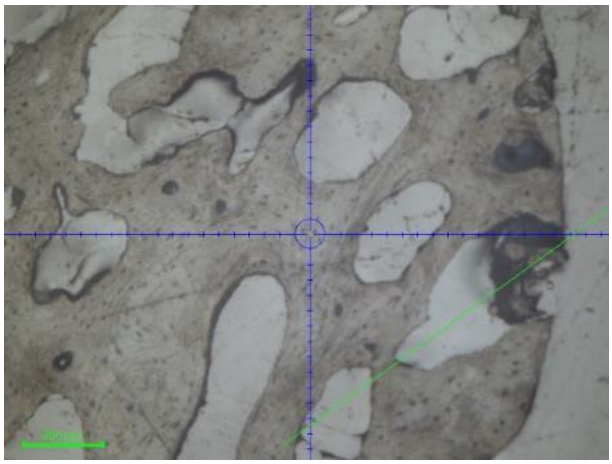

Figure 15: Light microscope image from blastic non organized tissue, Olympus CH-2, scale bar 200μm.

2.3.1 Nanoindentation procedure

In total, thirteen specimens from four donors were prepared to carry out the nanoindentation tests and they were divided in regions. Ten regions were identified for each specimen, and three indentations per region were performed using the TI 980 TriboIndenter (Fig.16) with a Berkovich tip.

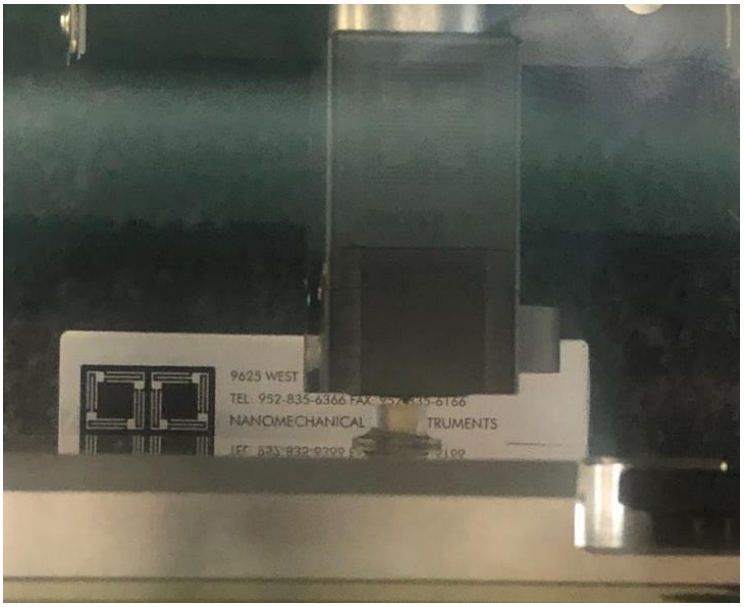

Figure 16: TI 980 TriboIndenter performing a nanoindentation on a specimen.

The nanoindentation tests followed the procedure implemented by the Sheffield University. The indentations were performed setting the following parameters (Fig.9):

- maximum load: 6000 μN
- loading rate: 300 μN/s (corresponding to a loading time of 20 s)
- holding time: 30 s (in order to reduce the consequences and the variability due to the creep)
- unloading rate: 902 μN/s (corresponding to a loading time of 6.65 s)

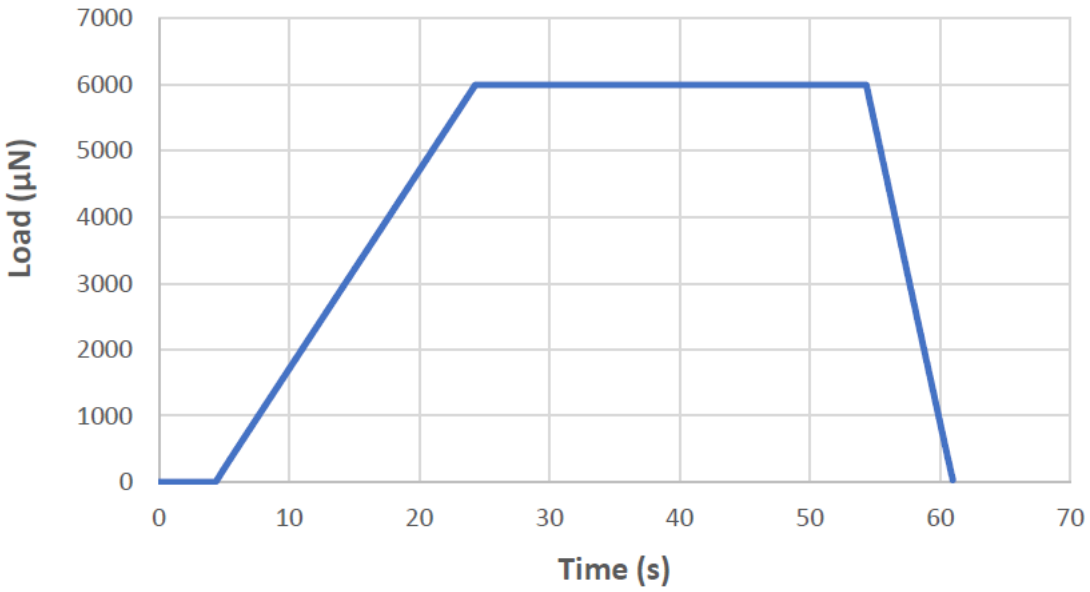

Figure 17: Load Function

2.3.2 Calibration procedure

In order to perform the calibration, the probe and the fused quartz sample were installed. A minimum of 25 indentations were performed on the standard sample.

The load function used for the calibration was a load control load function with a 5 seconds load time, a hold time of 2 seconds, followed by 5 seconds of unloading time. In order to calculate the computed area, it is important to know whether the indentation will be performed at a deep or shallow level.

After the indents have been completed, the area function was displayed. When the fit of the curve matches the range of values reported in the manual [11], the displayed area function was the area function applied to the system and the indenter can be moved to the bone specimens.

It is recommended to perform the nanoindentations only in the displacement range the probe was calibrated for.

2.4 Data analysis

A typical load-displacement curve (Fig.18) presents a toe at the beginning of the loading curve, which develops a concavity till the maximum load of 6000 µN, followed by an unloading curve.

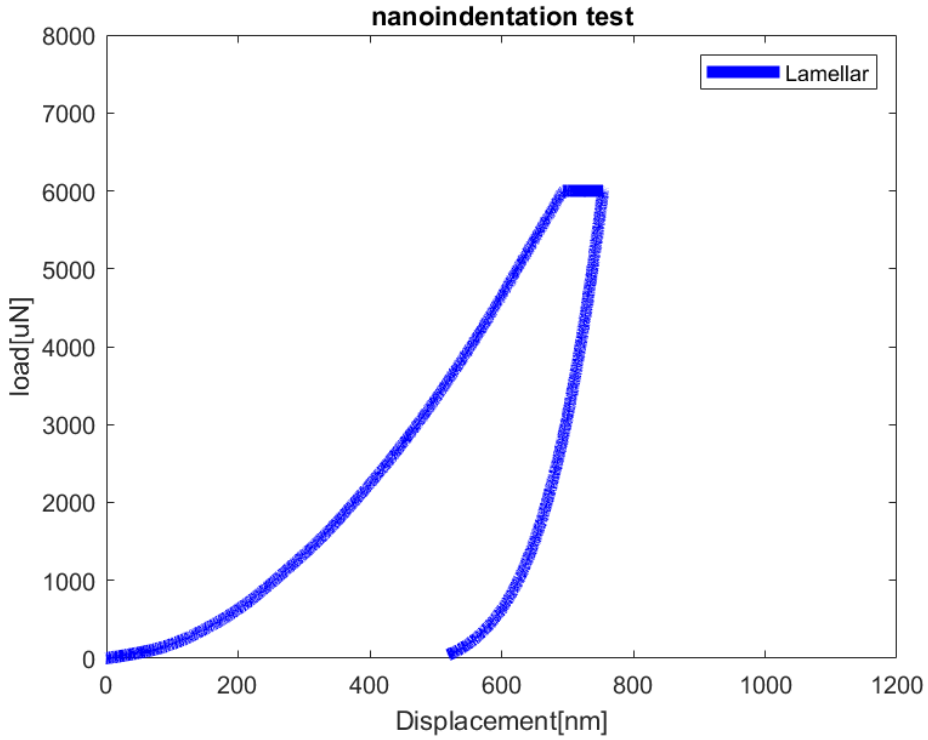

Figure 18: typical load-displacement curve obtained through the nanoindentation of a trabecular lamellar specimen.

Some curves showed a different shape because, as previously pointed out in the section 1.3, the accuracy of the instrument can be affected by many factors. Therefore, the wrong curves were excluded from the data analysis.

Through the analysis of the load-displacement curves, the local mechanical properties were determined referring to the theory discussed in the section 1.3. The parameters calculated for each nanoindentation were:

- Hardness (H)
- Elastic modulus (E_b)
- Indentation work (W)
- Elastic work (W_e)
- Dissipated work (W_d)

In particular, the formula to calculate the elastic modulus was derived by the relationship between the indentation modulus of rateindependent (nonviscous) materials reported in the section 1.3:

$$E = (1 - \nu^2)\, E_{ind}$$

Moreover, the values of the Poisson's ratio used to calculate E_{b1} and E_{b2} were 0.3 and 0.32 respectively.

2.5 Statistical analysis

The statistical analysis was performed in order to investigate how the presence of blastic metastases affects the local mechanical properties of the trabecular tissue with respect to the trabecular lamellar tissue, considering different population of tissue.

During the statistical analysis three types of tissue were distinguished according to their tissue appearance observed through the microscope:

- Trabecular lamellar tissue (highly organized tissue, with a healthy appearance)
- Blastic lamellar tissue (organized tissue)
- Blastic non organized tissue

The first statistical analysis was performed between the lamellar specimens (without any distinction between blastic and trabecular) and blastic non organized specimens.

Firstly, a Kolmogorov-Smirnov test assessed that the parameters obtained for the two distributions (lamellar and non organized tissue) were not normally distributed and the resulting p-value is reported in the Table 4:

Therefore, the non-parametric Mann-Whitney tests (significance threshold=0.05) were used to investigate if differences for each parameter exist.

Table 4: Kolmogorov-Smirnov test for lamellar and blastic parameters.

PARAMETER	LAMELLAR P-VALUE	BLASTIC P-VALUE
HARDNESS	$1.22\ 10^{-60}$	$1.29\ 10^{-46}$
ELASTIC MODULUS 1	$1.12\ 10^{-170}$	$4.29\ 10^{-126}$
ELASTIC MODULUS 2	$1.12\ 10^{-170}$	$4.29\ 10^{-126}$
INDENTATION WORK	$1.12\ 10^{-170}$	$4.29\ 10^{-126}$
ELASTIC ENERGY	$1.12\ 10^{-170}$	$4.29\ 10^{-126}$
DISSIPATED ENERGY	$1.12\ 10^{-170}$	$4.29\ 10^{-126}$

The second statistical analysis was performed between the blastic specimens (without any distinction between lamellar and non organized) and trabecular lamellar specimens.

Firstly, a Kolmogorov-Smirnov test assessed that the parameters obtained for the two groups (blastic and trabecular) were not normally distributed and the resulting p-value is reported in the Table 5:

Therefore, the non-parametric Mann-Whitney tests (significance threshold=0.05) were used to investigate potential statistically differences for each parameter.

Table 5: Kolmogorov-Smirnov test for trabecular and blastic parameters.

PARAMETER	TRABECULAR P-VALUE	BLASTIC P-VALUE
HARDNESS	$6.61\ 10^{-21}$	$5.85\ 10^{-88}$
ELASTIC MODULUS 1	$1.64\ 10^{-52}$	$4.89\ 10^{-244}$
ELASTIC MODULUS 2	$1.64\ 10^{-52}$	$4.89\ 10^{-244}$
INDENTATION WORK	$1.64\ 10^{-52}$	$4.89\ 10^{-244}$
ELASTIC ENERGY	$1.64\ 10^{-52}$	$4.89\ 10^{-244}$
DISSIPATED ENERGY	$1.64\ 10^{-52}$	$4.89\ 10^{-244}$

The last statistical analysis was performed between the trabecular lamellar, the blastic lamellar and the blastic non organized specimens.

Firstly, a Kolmogorov-Smirnov test assessed that the parameters obtained for the three groups (trabecular lamellar, blastic lamellar and blastic non organized) were not normally distributed and the resulting p-value is reported in the Table 6:

Therefore, the non-parametric Kruskal-Wallis test was used to investigate potential statistically differences for each parameter.

If the Kruskal-Wallis test evidenced any significant difference among the investigated parameters of the distributions, a Mann-Whitney test (significance threshold=0.05) was performed between the distributions under consideration, to carry out a Post Hoc analysis.

Table 6: Kolmogorov-Smirnov test for trabecular lamellar, blastic lamellar and blastic non organized parameters.

PARAMETER	TRABECULAR LAMELLAR P-VALUE	BLASTIC LAMELLAR P-VALUE	BLASTIC NON ORGANIZED P-VALUE
HARDNESS	$6.60\ 10^{-21}$	$8.23\ 10^{-43}$	$9.79\ 10^{-47}$
ELASTIC MODULUS 1	$1.64\ 10^{-52}$	$5.69\ 10^{-120}$	$4.29\ 10^{-126}$
ELASTIC MODULUS 2	$1.64\ 10^{-52}$	$5.69\ 10^{-120}$	$4.29\ 10^{-126}$
INDENTATION WORK	$1.64\ 10^{-52}$	$5.69\ 10^{-120}$	$4.29\ 10^{-126}$
ELASTIC ENERGY	$1.64\ 10^{-52}$	$5.69\ 10^{-120}$	$4.29\ 10^{-126}$
DISSIPATED ENERGY	$1.64\ 10^{-52}$	$5.69\ 10^{-120}$	$4.29\ 10^{-126}$

3. Results

In total, 335 nanoindentations were performed, excluding the thirty-four tests influenced by the errors mentioned in the section 1.3.

3.1 Mechanical properties lamellar and non organized tissue

Significant difference was found between the lamellar specimens and the blastic non organized specimens, in terms of hardness and elastic modulus (p-value<0.05, Table 7 and Fig.19), while no significant difference was found in terms of indentation work, elastic work and dissipated work. Data is reported as mean ± standard deviation in the Table 8.

Table 7: p-values lamellar vs blastic non organized specimens.

PARAMETER	LAMELLAR VS BLASTIC P-VALUE
HARDNESS	0.026
ELASTIC MODULUS 1	0.028
ELASTIC MODULUS 2	0.028
INDENTATION WORK	0.080
ELASTIC ENERGY	0.336
DISSIPATED ENERGY	0.132

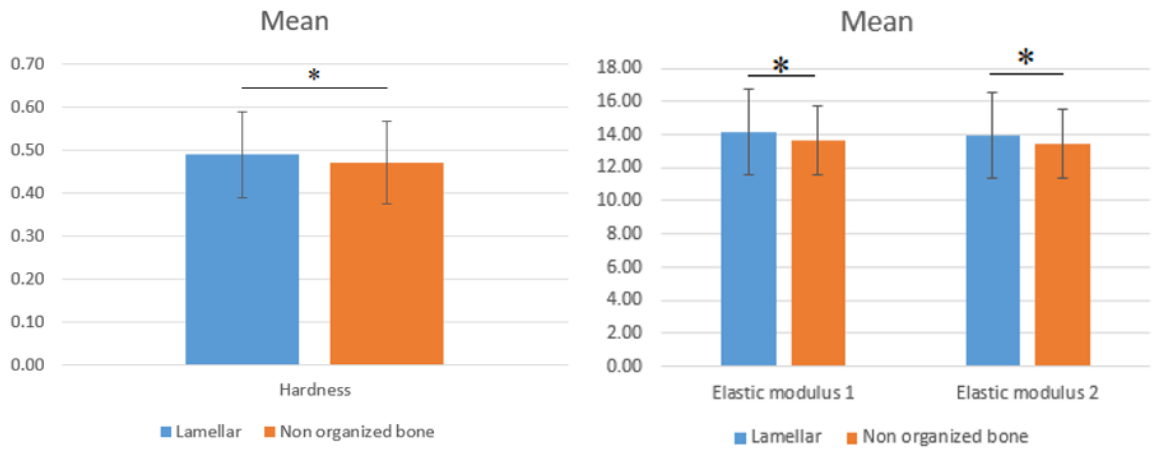

Fig.19: Hardness and elastic modulus for lamellar and non organized tissue. Error bars represent standard deviations. * indicates p<0.05.

Table 8: mean ± standard deviation of parameters for lamellar and blastic non organized specimens.

PARAMETERS	LAMELLAR TISSUE	BLASTIC TISSUE
HARDNESS	0.49 ± 0.10 (GPa)	0.47 ± 0.10 (GPa)
ELASTIC MODULUS 1	14.16 ± 2.59 (GPa)	13.66 ± 2.11 (GPa)
ELASTIC MODULUS 2	13.96 ± 2.55 (GPa)	13.48 ± 2.08 (GPa)
INDENTATION WORK	1770761.52 ± 198408.46 (fNm)	1799513.75 ± 171107.36 (fNm)
ELASTIC ENERGY	429817.94 ± 67030.53 (fNm)	433284.51 ± 50573.10 (fNm)
DISSIPATED ENERGY	1340943.58 ± 178543.16 (fNm)	1366229.24 ± 163730.99 (fNm)

3.2 Mechanical properties trabecular and blastic tissue

No significant differences were found between the parameters of trabecular tissue and blastic (without any distinction between the lamellar and non organized) tissue (Table 9). Data is reported as mean ± standard deviation in the Table 10.

Table 9: p-values trabecular vs blastic specimens.

PARAMETER	TRABECULAR VS BLASTIC P-VALUE
HARDNESS	0.407
ELASTIC MODULUS 1	0.206
ELASTIC MODULUS 2	0.206
INDENTATION WORK	0.074
ELASTIC ENERGY	0.834
DISSIPATED ENERGY	0.100

Table 10: mean ± standard deviation of parameters for trabecular lamellar and blastic specimens.

PARAMETERS	TRABECULAR LAMELLAR TISSUE	BLASTIC TISSUE
HARDNESS	0.49 ± 0.09 (GPa)	0.48 ± 0.10 (GPa)
ELASTIC MODULUS 1	14.22 ± 2.59 (GPa)	13.89 ± 2.37 (GPa)
ELASTIC MODULUS 2	14.03 ± 2.56 (GPa)	13.70 ± 2.34 (GPa)
INDENTATION WORK	1750449.01 ± 175927.54 (fNm)	1789754.09 ± 189543.48 (fNm)
ELASTIC ENERGY	434163.56 ± 79833.09 (fNm)	430685.11 ± 55834.38 (fNm)
DISSIPATED ENERGY	1316285.45 ± 150241.75 (fNm)	1359068.98 ± 176297.47 (fNm)

3.3 Mechanical properties trabecular lamellar, blastic lamellar and blastic non organized tissue

Significant difference was found between the blastic lamellar specimens and the blastic non organized specimens, in terms of hardness (p-value<0.05, Table 11, Table 12, Table 13 and Fig.20). Moreover, significant difference was observed between the indentation work of trabecular lamellar specimens and blastic non organized specimens (p-value<0.05, Table 10 and Fig.21). Data is reported as mean ± standard deviation in the Table 14.

Table 11: p-values trabecular lamellar vs blastic lamellar specimens.

PARAMETER	TRABECULAR LAMELLAR VS BLASTIC LAMELLAR P-VALUE
HARDNESS	0.969
ELASTIC MODULUS 1	0.692
ELASTIC MODULUS 2	0.689
INDENTATION WORK	0.269
ELASTIC ENERGY	0.612
DISSIPATED ENERGY	0.249

Table 12: p-values trabecular lamellar vs blastic non organized specimens.

PARAMETER	TRABECULAR LAMELLAR VS BLASTIC NON ORGANIZED P-VALUE
HARDNESS	0.125
ELASTIC MODULUS 1	0.057
ELASTIC MODULUS 2	0.058
INDENTATION WORK	0.031
ELASTIC ENERGY	0.915
DISSIPATED ENERGY	0.062

Table 13: p-values blastic lamellar vs blastic non organized specimens.

PARAMETER	BLASTIC LAMELLAR VS BLASTIC NON ORGANIZED P-VALUE
HARDNESS	0.042
ELASTIC MODULUS 1	0.068
ELASTIC MODULUS 2	0.068
INDENTATION WORK	0.273
ELASTIC ENERGY	0.228
DISSIPATED ENERGY	0.347

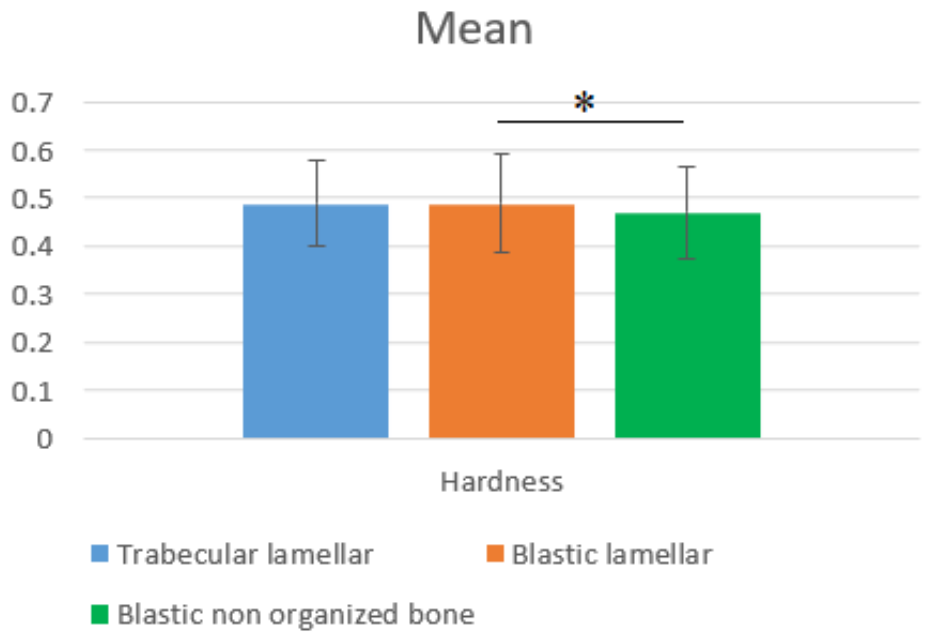

Fig.20: Hardness of trabecular lamellar, blastic lamellar and blastic non organized tissue. Error bars represent standard deviations. * indicates $p<0.05$.

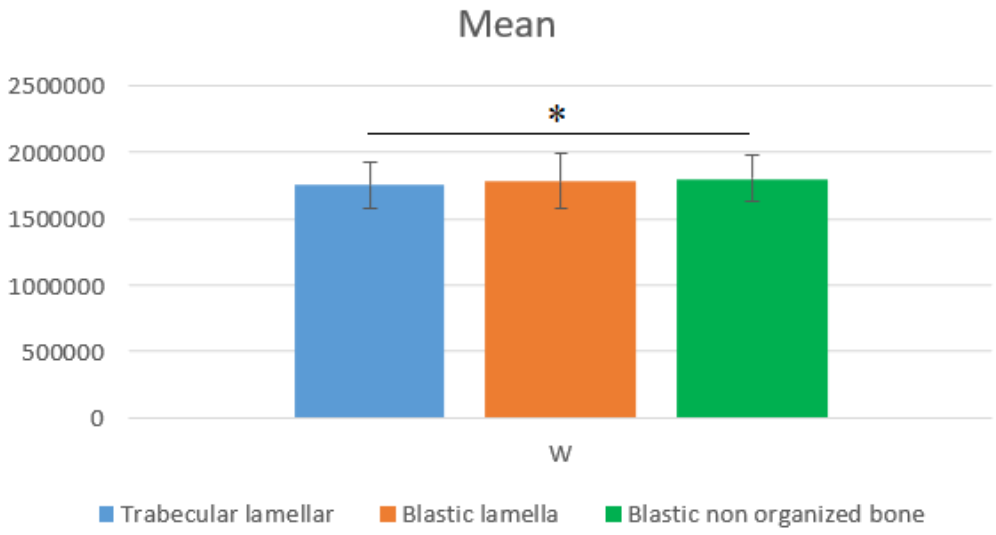

Fig.21: Indentation work of trabecular lamellar, blastic lamellar and blastic non organized tissue. Error bars represent standard deviations. * indicates $p<0.05$.

Table 14: mean ± standard deviation of parameters for trabecular lamellar and blastic lamellar and blastic non organized specimens.

PARAMETERS	TRABECULAR LAMELLAR TISSUE	BLASTIC LAMELLAR TISSUE	BLASTIC NON ORGANIZED TISSUE
HARDNESS	0.49 ± 0.09 (GPa)	0.49 ± 0.10 (GPa)	0.47 ± 0.10 (GPa)
ELASTIC MODULUS 1	14.22 ± 2.59 (GPa)	14.13 ± 2.60 (GPa)	13.66 ± 2.11 (GPa)
ELASTIC MODULUS 2	14.03 ± 2.56 (GPa)	13.94 ± 2.56 (GPa)	13.48 ± 2.08 (GPa)
INDENTATION WORK	1750449.01 ± 175927.54 (fNm)	1779488.38 ± 207326.01 (fNm)	1799513.75 ± 171107.36 (fNm)
ELASTIC ENERGY	434163.56 ± 79833.09 (fNm)	427950.94 ± 60951.93 (fNm)	433284.51 ± 50573.10 (fNm)
DISSIPATED ENERGY	1316285.45 ± 150241.75 (fNm)	1351537.44 ± 188937.66 (fNm)	1366229.24 ± 163730.99 (fNm)

3.3.1 Correlations between mechanical properties and elastic modulus of trabecular lamellar, blastic lamellar and blastic non organized tissue

Statistical analysis were performed to investigate the correlations between the elastic modulus and the mechanical properties, hardness, total work, elastic work and dissipated work.

Significant correlations were found between the elastic modulus of all the specimens and the other mechanical properties of the specimens, with different dispersion coefficients (Table 15, Figure 21):

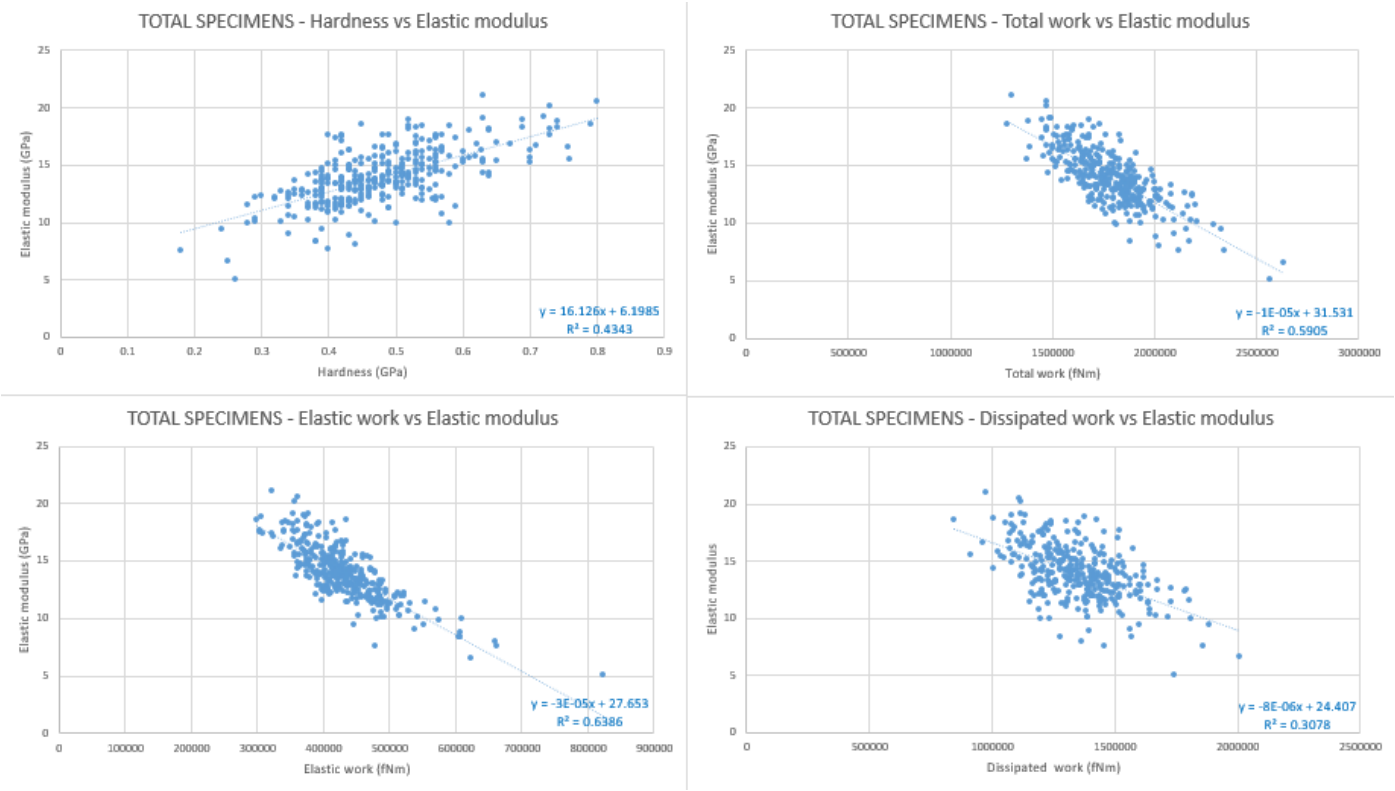

Figure 21: correlation between elastic modulus and the others mechanical parameters of the total specimens.

Table 15: p-values of the correlation between elastic modulus and the others mechanical parameters of the total specimens.

TOTAL SPECIMENS	p-values
Hardness vs Elastic modulus	$4.2047 \cdot 10^{-43}$
Total work vs Elastic modulus	$1.5705 \cdot 10^{-66}$
Elastic work vs Elastic modulus	$1.3989 \cdot 10^{-75}$
Dissipated work vs Elastic modulus	$1.9518 \cdot 10^{-28}$

Significant correlations were found between the elastic modulus and the other mechanical properties of the trabecular lamellar specimens, with different dispersion coefficients (Figure 22, Table 16):

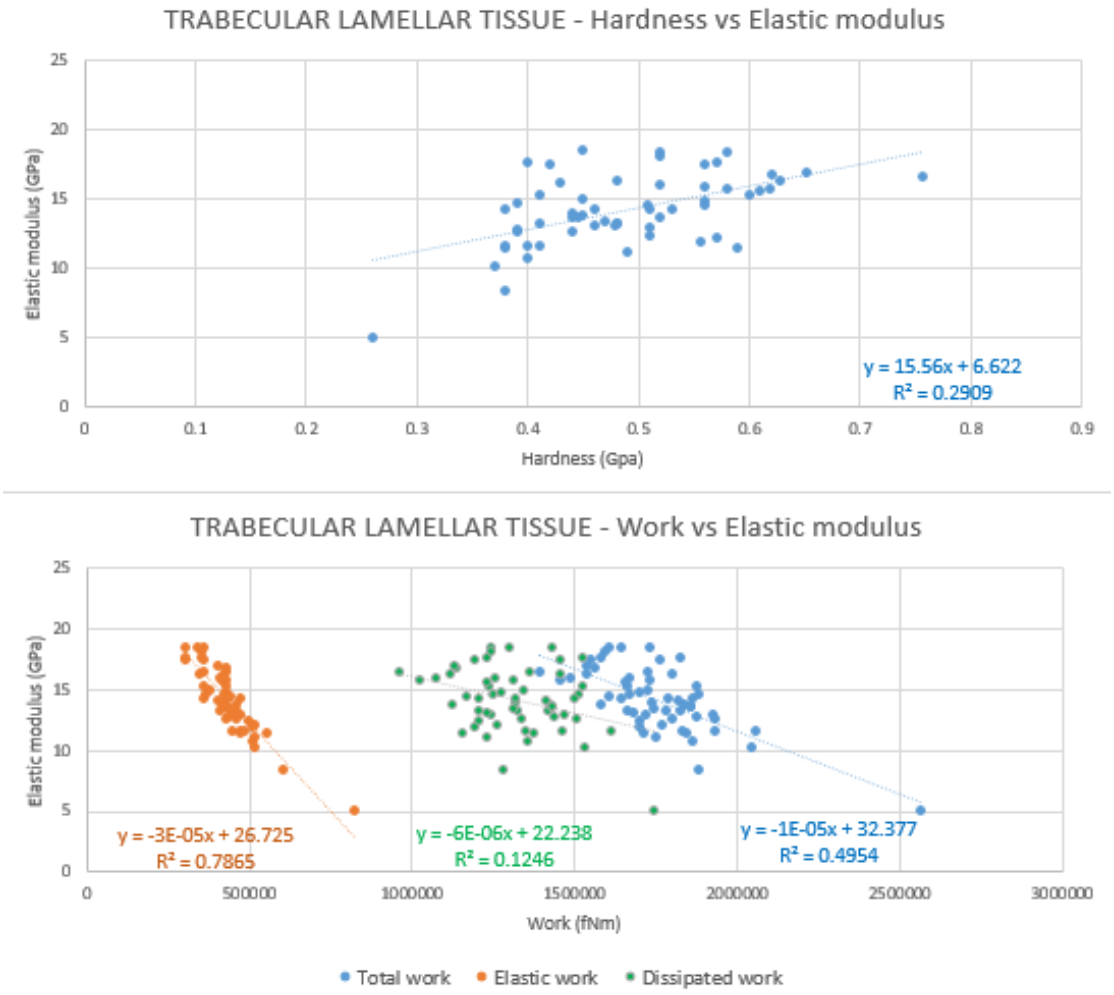

Figure 22: correlation between elastic modulus and the others mechanical parameters of the trabecular lamellar specimens.

Table 16: p-values of the correlation between elastic modulus and the others mechanical parameters of the trabecular lamellar specimens.

TRABECULAR LAMELLAR SPECIMENS	p-values
Hardness vs Elastic modulus	$1.2483 \cdot 10^{-5}$
Total work vs Elastic modulus	$7.1362 \cdot 10^{-10}$
Elastic work vs Elastic modulus	$1.9876 \cdot 10^{-20}$
Dissipated work vs Elastic modulus	$6.5787 \cdot 10^{-3}$

Significant correlations were found between the elastic modulus and the other mechanical properties of the blastic lamellar specimens, with different dispersion coefficients (Figure 23, Table 17).

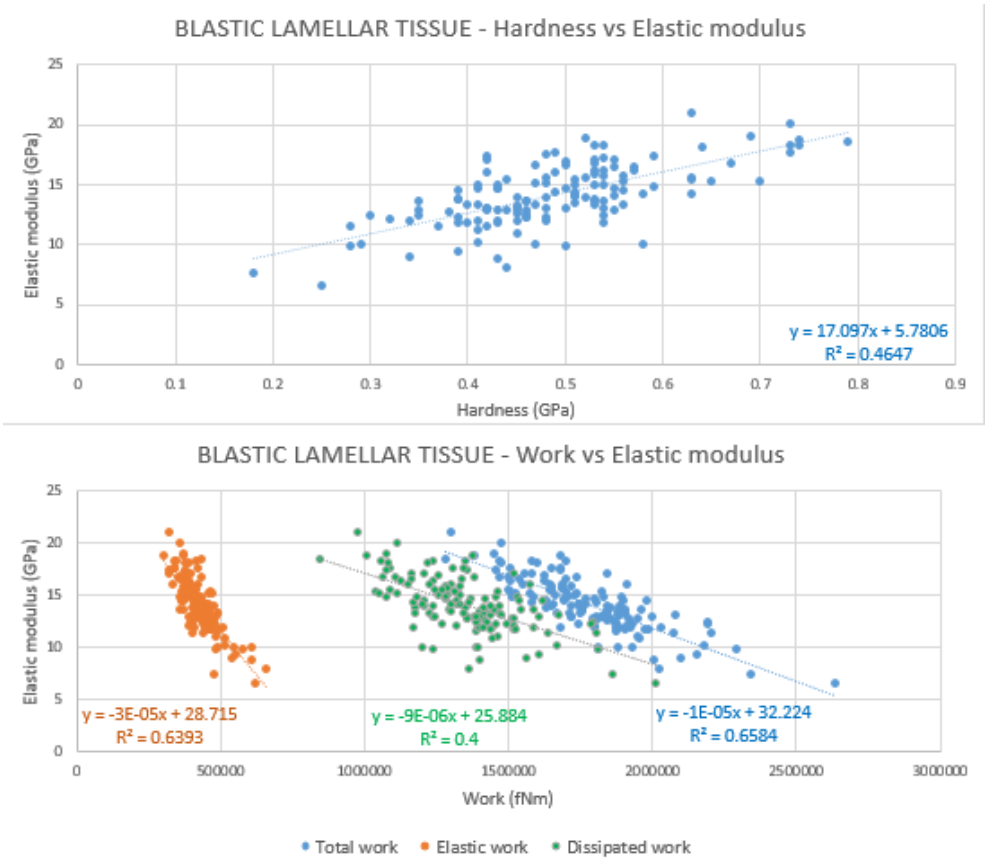

Figure 23: correlation between elastic modulus and the others mechanical parameters of the blastic lamellar specimens.

Table 17: p-values of the correlation between elastic modulus and the others mechanical parameters of the blastic lamellar specimens.

BLASTIC LAMELLAR SPECIMENS	p-values
Hardness vs Elastic modulus	$9.0130 \cdot 10^{-20}$
Total work vs Elastic modulus	$8.0059 \cdot 10^{-33}$
Elastic work vs Elastic modulus	$3.0358 \cdot 10^{-31}$
Dissipated work vs Elastic modulus	$1.9032 \cdot 10^{-16}$

Significant correlations were found between the elastic modulus and the other mechanical properties of the blastic non organized specimens, with different dispersion coefficients (Figure 24, Table 18).

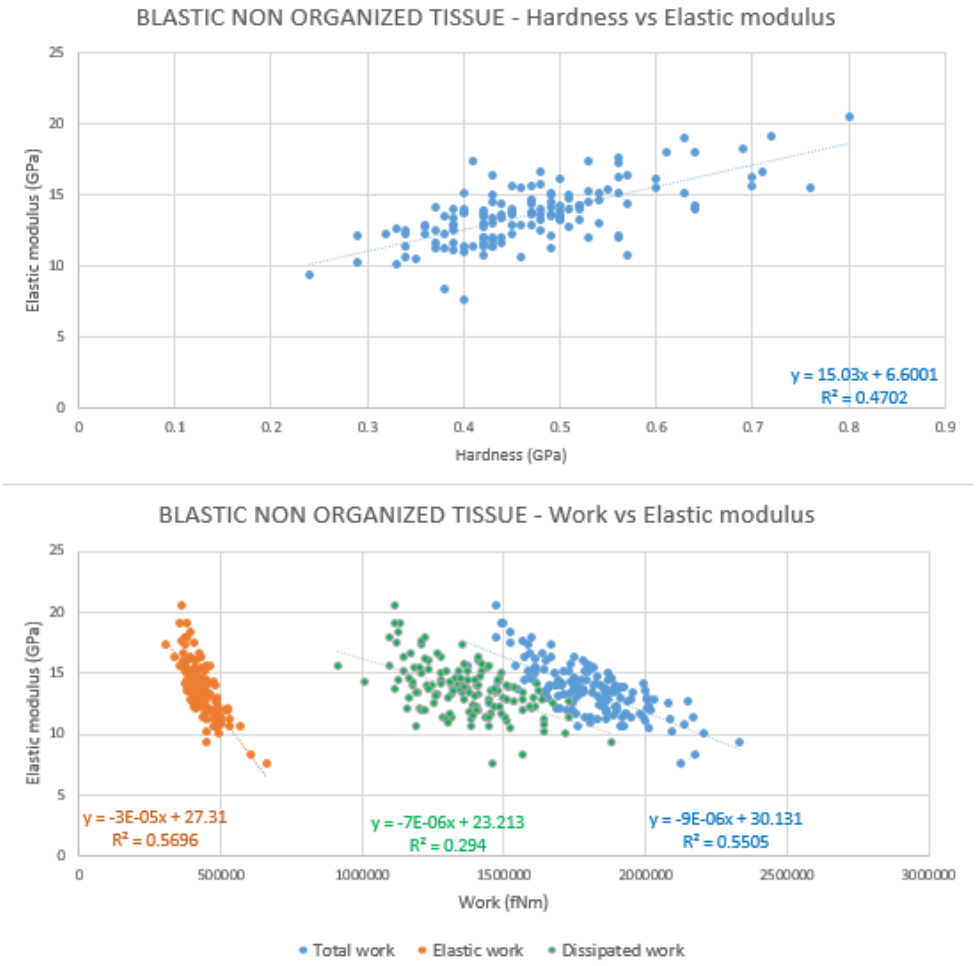

Figure 24: correlation between elastic modulus and the others mechanical parameters of the blastic non organized specimens.

Table 18: p-values of the correlation between elastic modulus and the others mechanical parameters of the blastic non organized specimens.

BLASTIC NON ORGANIZED SPECIMENS	p-values
Hardness vs Elastic modulus	$4.7293 \cdot 10^{-21}$
Total work vs Elastic modulus	$4.4388 \cdot 10^{-26}$
Elastic work vs Elastic modulus	$2.0894 \cdot 10^{-27}$
Dissipated work vs Elastic modulus	$3.1711 \cdot 10^{-12}$

4. Discussion

From the x-ray analysis it is not possible to assess how the local mechanical behaviour of the trabeculae is influenced by the presence of blastic metastases. Moreover, the blastic tissue has a high contrast radiographical appearance, which suggests a higher mineral density. However, it was noticed that the presence of blastic metastases is associated to an increased risk of fracture [6]. Therefore, it is necessary to analyse the vertebral tissue at a sub-structural level, providing mechanical properties of the materials, such as elastic modulus, hardness and work values.

Starting from this paradigm, a series of scientific papers introduced these properties at micro- and nano- structural level, in healthy and metastatic vertebral tissue. In "*Tissue properties of the human vertebral body sub-structures evaluated by means of microindentation"* Dall'Ara et al. [5] extracted six healthy human lumbar vertebrae from six donors and analysed them at the microscale level. A preliminary information about the indentation modulus was obtained at this dimensional scale, highlighting the micro behaviour of the tissue and introducing the need to investigate the mechanical properties at the level of the individual lamella. To this aim, we used nanoindentation technique to analyse both healthy and metastatic vertebral tissue. Concerning the healthy tissue, the values of hardness and elastic modulus from two healthy thoracic vertebrae (T12) were obtained by Rho et al. [22] in "*Elastic properties of human cortical and trabecular lamellar bone measured by nanoindentation"*. Nevertheless, our main interest is in understanding the mechanical behaviour of vertebral tissue affected by a non-physiological remodelling as in presence of blastic metastases. In this respect, Stadelmann et al. [26] were the only that evaluated the mechanical properties of the blastic vertebral tissue in "*Conventional finite element models estimate the strength of metastatic human vertebrae despite alterations of the bone's tissue and structure"*. In this paper, the values of the indentation modulus and the dissipated work – total work ratio were obtained from twelve blastic specimens through a nanoindentation procedure.

This scenario is not fully comprehensive to understand the local mechanical behaviour of the trabeculae when influenced by the presence of blastic metastases. In order to obtain a more complete overview, in this study 13 bone cores were prepared from lumbar vertebrae of four male donors (Table 3). Regions with healthy trabecular, blastic lamellar, and blastic non organized tissue were identified through an optical microscope. The different tissues were subjected to a nanoindentation procedure to measure the hardness, the elastic modulus, the total work, the elastic work and the dissipated work of the metastatic tissue.

The hardness and the elastic modulus resulted to be lower than 4.1% and 3.5%, respectively in the blastic non organized bone when it was compared to lamellar tissue. This is in line with the expected composition of non organized bone tissue, since it contains a lower hydroxyapatite (HA) concentration [2]. Indeed, HA is directly associated with bone tissue stiffness [2], therefore a lower degree of mineralization in the non organized bone could be associated to a lower hardness. Similarly, the hardness resulted to be lower than 4.1% when blastic lamellar tissue and blastic non organized tissue were compared, while unexpectedly no significant difference was observed in terms of elastic modulus, although both the hardness and the elastic modulus should be related to the HA concentration. Therefore, correlation analysis was performed in order to understand if the elastic modulus was related to the hardness.

Correlation between elastic modulus and the other mechanical properties showed that the elastic modulus (with or without any classification based on the tissue appearance) resulted to be correlated to the other mechanical properties (section 3.3.1). In particular, the significant correlation in the case of blastic lamellar and blastic non organized tissue, shows that also the elastic modulus is related to the hardness, therefore it may be related to HA concentration, too. Hence, a relationship with the HA concentration can be expected also in this case.

The values of the elastic modulus obtained in our study resulted to be higher when compared with those of the reference paper by Dall'Ara et al. [5]. Indeed, as shown in Table 19, there is a difference of +12.31% (Elastic modulus=12.47 GPa in Dall'Ara et al.; Elastic modulus=14.22 GPa in our study). This is probably due to the indentation performed at a different dimensional scale, since we used the nanoindentation technique while Dall'Ara et al. used the microindentation technique. Indeed, the microindentation technique was performed with a maximal depth of 2.5 μm, a loading rate of 60 mN/min and a holding time of 60 s, followed by an unloading rate equal to that used during the loading. Furthermore, the specimens tested by Dall'Ara et al. were obtained from healthy vertebrae, while we compared those values to metastatic vertebrae with a healthy appearance.

Table 19: Comparison between the values of elastic modulus found in Dall'Ara et al. and in our study for trabecular lamellar specimens.

	Dall'Ara et al.	Our study	Difference
Elastic modulus (GPa)	12.47*	14.22±2.59	+12.31%

*in this study only the indentation modulus was reported, consequently the elastic modulus was calculated by using the formula reported in the section 1.3.

Moreover, the values of hardness and elastic modulus obtained in our study resulted to be higher also when compared with those of the reference paper by Rho et al. [22]. As reported in Table 20, there is a difference of +4.29% relating to the hardness and a difference of +5.77% relating to the elastic modulus (Hardness=0.468 GPa in Rho et al.; Hardness=0.489 GPa in our study; Elastic modulus=13.4 GPa in Rho et al.; Elastic modulus=14.22 GPa in our study). This is probably due to the different indentation parameters. Indeed, in the reference paper, the specimens were tested with an indentation depth of 1000 nm, a loading rate of 750 μNs^{-1}, a holding time of 10 seconds, followed by an unloading rate equal to half that used during the loading. Moreover, the specimens tested by Rho et al. came from healthy vertebrae, while we tested tissues of metastatic vertebrae with a healthy appearance. In addition, the specimens indented by Rho et al. were obtained from thoracic vertebrae (T12), while in our study we considered specimens obtained from lumbar vertebrae (L1, L2, L4). The different vertebral level, as reported by Giambini et al. [10], may affect the mechanical properties of the tissue.

Table 20: Comparison between the values of hardness and elastic modulus found in Rho et al. and in our study for trabecular lamellar specimens.

	Rho et al.	Our study	Difference
Hardness (GPa)	0.468 ± 0.079	0.489±0.090	+4.29%
Elastic modulus (GPa)	13.4 ± 2.0	14.22±2.59	+5.77%

In addition, the values of elastic modulus obtained in our study resulted to be higher also when they were compared to the reference paper by Stadelmann et al. [26]. Indeed, as shown in Table 21, there is a difference of +17.28% (Elastic modulus=11.3 GPa in Stadelmann et al.; Elastic modulus=14.22 GPa in our study). This is probably due to the fact that the indentation parameters were different. In fact, in the reference paper, the specimens were tested with an indentation depth of 1000nm, a loading rate of 100 $mNmin^{-1}$, a holding time of 30 seconds, followed by an unloading rate of 400$mNmin^{-1}$.

Finally, since we expect the work to be related to the collagen structure, it was also analysed. The total work resulted to be higher than 2.8% in the blastic non organized tissue when it was compared to trabecular lamellar tissue. This is in line with the expected structure of non organized bone tissue, since collagen mutations can affect the organization of the collagen fibrils [1]. Since the content and maturity of the collagen is directly associated with the toughness [2], this could explain the greater compliance shown by the blastic non organized tissue. Furthermore, as shown in Table 21, the values of the dissipated work - total work ratio resulted to be in line with those reported by Stadelmann et al. (Wd/W=0.77 in Stadelmann et al.; Wd/W=0.76 in our study).

Table 21: Comparison between the values of elastic modulus found in Stadelmann et al. and in our study for blastic specimens.

	Stadelmann et al.	Our study	Difference
Elastic modulus (GPa)	11.30*	13.66±0.10	+17.28%
Wd/W	0.77	0.76	-1.32%

*in this study only the indentation modulus was reported, consequently the elastic modulus was calculated by using the formula reported in the section 1.3.

4.1 Limitations of the study

This study has few limitations. The first one is the sample size: 13 specimens were obtained from four donors. A larger sample size, both in terms of specimens and donors, should be tested to confirm the preliminary findings observed in this study.

Assessment of blastic or healthy tissue was based on radiographical appearance. A histochemical analysis should be performed in order to confirm the radiographical assessment and finally properly assess the tissue under investigation.

Furthermore, although the radiological appearance of blastic tissue suggests the presence of a higher level of mineral content in the extracellular matrix, the noticed increased risk of fracture [6], suggests the presence of a lower degree of mineralization and an increased content of collagen, which is not properly organized. In order to confirm this hypothesis, further studies may perform a histochemical analysis to investigate the composition of the blastic tissue.

The comparison performed between blastic and trabecular lamellar tissue showed no significant differences in terms of mechanical properties. These results do not suggest that potential differences between the two types of tissue exist at a different dimensional scale. Indeed, differences between blastic and trabecular lamellar tissue may lie at the level of the collagen structure. Therefore, further studies could investigate the mechanical properties of the analysed specimens at a different level. Indeed, morphometric measurements may be assessed through immunohistochemical analysis, in order to assess whether the orientation of the collagen fibers could affect the mechanical properties of the metastatic tissue.

5. Conclusions

In this study, the nanoindentation technique was used to investigate the potential differences in terms of mechanical properties of vertebral tissue affected/not affected by blastic metastases. To this aim, nanoindentations were performed on specimens obtained from donors with vertebral blastic metastases in order to measure hardness, elastic modulus, total work, elastic work and dissipated work. The selected specimens were classified in trabecular lamellar tissue, blastic lamellar tissue and blastic non organized bone tissue, according to the appearance of their tissue under the microscope.

The outcomes showed significant differences in terms of mechanical properties between blastic non organized bone tissue and lamellar bone tissue. Indeed, the hardness and the elastic modulus resulted to be lower in the non organized bone tissue when it was compared to lamellar tissue. This is in line with the expected lower degree of mineralization in the non organized bone tissue. Similarly, the hardness resulted to be lower in the non organized bone tissue when it was compared to blastic lamellar tissue. Although both the hardness and the elastic modulus should be related to the HA concentration, unexpectedly, no significant difference was observed in terms of elastic modulus. Therefore, correlation analysis was performed in order to understand if the elastic modulus was related to the hardness. Moreover, the total work resulted to be higher in the blastic non organized bone tissue when it was compared to the trabecular lamellar tissue. This result suggests the expected content and different organization of the collagen fibrils in the non organized bone tissue. Furthermore, the results obtained from trabecular lamellar specimens were higher than the values found in literature in terms of elastic modulus and hardness. The results obtained from blastic specimens were higher than the values found in literature in terms of elastic modulus, while they were in line with literature in terms of dissipated work – total work ratio. Since no significant differences were found between blastic tissue and trabecular lamellar tissue, further studies could investigate the mechanical properties of the analysed specimens at a different level.

In conclusion, the outcomes of this study highlight the importance of investigating the local mechanical properties of blastic tissue in order to understand to what extent its mechanical competence is modified.

References

[1] Alliston, T. (2014). Biological Regulation of Bone Quality. *Current osteoporosis reports*, *12*(3), 366–375. https://doi.org/10.1007/s11914-014-0213-4

[2] Bailey, S., Hackney, D., Vashishth, D., & Alkalay, R. N. (2020). The effects of metastatic lesion on the structural determinants of bone: Current clinical and experimental approaches. *Bone*, *138*, 115159. https://doi.org/10.1016/j.bone.2019.115159

[3] Cavazzoni, G. *In vitro characterization of the three-dimensional strain pattern in human vertebrae affected by metastases* [Tesi di laurea]

[4] Costa, M. C., Eltes, P., Lazary, A., Varga, P. P., Viceconti, M., & Dall'Ara, E. (2019). Biomechanical assessment of vertebrae with lytic metastases with subject-specific finite element models. *Journal of the Mechanical Behavior of Biomedical Materials*, *98*, 268–290. https://doi.org/10.1016/j.jmbbm.2019.06.027

[5] Dall'Ara E., Karl C., Mazza G., Franzoso G., Vena P., Pretterklieber M., Pahr D., Zysset P., Tissue properties of the human vertebral body sub-structures evaluated by means of microindentation.

[6] Donnelly, E. (2011). Methods for Assessing Bone Quality: A Review. *Clinical Orthopaedics and Related Research*, *469*(8), 2128–2138. https://doi.org/10.1007/s11999-010-1702-0

[7] Fisher, C. G., DiPaola, C. P., Ryken, T. C., Bilsky, M. H., Shaffrey, C. I., Berven, S. H., Harrop, J. S., Fehlings, M. G., Boriani, S., Chou, D., Schmidt, M. H., Polly, D. W., Biagini, R., Burch, S., Dekutoski, M. B., Ganju, A., Gerszten, P. C., Gokaslan, Z. L., Groff, M. W., … Fourney, D. R. (2010). A novel classification system for spinal instability in neoplastic disease: An evidence-based approach and expert consensus from the Spine Oncology Study Group. *Spine*, *35*(22), E1221-1229. https://doi.org/10.1097/BRS.0b013e3181e16ae2

[8] Fisher, C. G., Schouten, R., Versteeg, A. L., Boriani, S., Varga, P. P., Rhines, L. D., Kawahara, N., Fourney, D., Weir, L., Reynolds, J. J., Sahgal, A., Fehlings, M. G., & Gokaslan, Z. L. (2014). Reliability of the Spinal Instability Neoplastic Score (SINS) among radiation oncologists: An assessment of instability secondary to spinal metastases. *Radiation Oncology (London, England)*, *9*, 69. https://doi.org/10.1186/1748-717X-9-69

[9] Fisher, C. G., Versteeg, A. L., Schouten, R., Boriani, S., Varga, P. P., Rhines, L. D., Heran, M. K. S., Kawahara, N., Fourney, D., Reynolds, J. J., Fehlings, M. G., & Gokaslan, Z. L. (2014). Reliability of the spinal instability neoplastic scale among radiologists: An assessment of instability secondary to spinal metastases. *AJR. American Journal of Roentgenology*, *203*(4), 869–874. https://doi.org/10.2214/AJR.13.12269

[10] Fonseca, H., Moreira-Gonçalves, D., Coriolano, H.-J. A., & Duarte, J. A. (2014). Bone quality: The determinants of bone strength and fragility. *Sports Medicine (Auckland, N.Z.)*, *44*(1), 37–53. https://doi.org/10.1007/s40279-013-0100-7

[11] Giambini, H., Wang, H.-J., Zhao, C., Chen, Q., Nassr, A., & An, K.-N. (2013). Anterior and posterior variations in mechanical properties of human vertebrae measured by nanoindentation. *Journal of Biomechanics*, *46*(3), 456–461. https://doi.org/10.1016/j.jbiomech.2012.11.008

[12] Hysitron. (s.d.). *TI 980 TriboIndenter User Manual*.

[13] Jakes, Joseph E., *Improved methods for nanoindentation Berkovich probe calibrations using fused silica | SpringerLink*. (s.d.). , da https://link.springer.com/article/10.1007/s10853-017-1922-8

[14] Kampschulte, M., Langheinirch, A., Sender, J., Litzlbauer, H., Althöhn, U., Schwab, J., Alejandre-Lafont, E., Martels, G., & Krombach, G. (2016). Nano-Computed Tomography: Technique and Applications. *RöFo - Fortschritte Auf Dem Gebiet Der Röntgenstrahlen Und Der Bildgebenden Verfahren*, *188*(02), 146–154. https://doi.org/10.1055/s-0041-106541

[15] Khoury, B. M., Bigelow, E. M. R., Smith, L. M., Schlecht, S. H., Scheller, E. L., Andarawis-Puri, N., & Jepsen, K. J. (2015). The use of nano-computed tomography to enhance musculoskeletal research. *Connective tissue research*, *56*(2), 106–119. https://doi.org/10.3109/03008207.2015.1005211

[16] Laufer, I., Rubin, D. G., Lis, E., Cox, B. W., Stubblefield, M. D., Yamada, Y., & Bilsky, M. H. (2013). The NOMS framework: Approach to the treatment of spinal metastatic tumors. *The Oncologist*, *18*(6), 744–751. https://doi.org/10.1634/theoncologist.2012-0293

[17] Nater, A., Sahgal, A., & Fehlings, M. (2018). Management—Spinal metastases. *Handbook of Clinical Neurology*, *149*, 239–255. https://doi.org/10.1016/B978-0-12-811161-1.00016-5

[18] Palanca, M., Barbanti-Bròdano, G., Marras, D., Marciante, M., Serra, M., Gasbarrini, A., Dall'Ara, E., & Cristofolini, L. (2021). Type, size, and position of metastatic lesions explain the deformation of the vertebrae under complex loading conditions. *Bone*, *151*, 116028. https://doi.org/10.1016/j.bone.2021.116028

[19] Pepe, V., *DEVELOPMENT OF PROCEDURES TO PERFORM NANOINDENTATION TESTS ON DIFFERENT BONE STRUCTURES*, [Tesi di Laurea]

[20] Peyrin, F., Dong, P., Pacureanu, A., & Langer, M. (2014). Micro- and nano-CT for the study of bone ultrastructure. *Current Osteoporosis Reports*, *12*(4), 465–474. https://doi.org/10.1007/s11914-014-0233-0

[21] Piccioli, A., Campanacci, D. A., Daolio, P., Gasbarrini, A., Ippolito, V., Maccauro, G., Piana,

R., Ruggieri, P., Spinelli, M. S., Capanna, R., & Ibrahim, T. (s.d.). *Linee guida TRATTAMENTO DELLE METASTASI OSSEE*

[22] Rho Jae-Young, Tsui Ting Y., Pharr George M., Elastic properties of human cortical and trabecular lamellar bone measured by nanoindentation

[23] Roodman, G. David, *Mechanisms of Bone Metastasis | NEJM*. (s.d.). , da https://www.nejm.org/doi/full/10.1056/nejmra030831

[24] Ryan, C., Stoltzfus, K. C., Horn, S., Chen, H., Louie, A. V., Lehrer, E. J., Trifiletti, D. M., Fox, E. J., Abraham, J. A., & Zaorsky, N. G. (2022). Epidemiology of bone metastases. *Bone*, *158*, 115783. https://doi.org/10.1016/j.bone.2020.115783

[25] Shah, L. M., & Salzman, K. L. (2011). Imaging of spinal metastatic disease. *International Journal of Surgical Oncology*, *2011*, 769753. https://doi.org/10.1155/2011/769753

[26] Stadelmann, M. A., Schenk, D. E., Maquer, G., Lenherr, C., Buck, F. M., Bosshardt, D. D., Hoppe, S., Theumann, N., Alkalay, R. N., & Zysset, P. K. (2020). Conventional finite element models estimate the strength of metastatic human vertebrae despite alterations of the bone's tissue and structure. *Bone*, *141*, 115598. https://doi.org/10.1016/j.bone.2020.115598

[27] Steinberger Jeremy M., Yuk Frank, Doshi Amish H., Green Sheryl, Germano Isabelle M., Multidisciplinary management of metastatic spine disease: initial symptom-directed management

[28] Tomasian, A., & Jennings, J. W. (2020). Vertebral Metastases: Minimally Invasive Percutaneous Thermal Ablation. *Techniques in Vascular and Interventional Radiology*, *23*(4), 100699. https://doi.org/10.1016/j.tvir.2020.100699

[29] Zysset, P. K. (2009). Indentation of bone tissue: A short review. *Osteoporosis International: A Journal Established as Result of Cooperation between the European Foundation for Osteoporosis and the National Osteoporosis Foundation of the USA*, *20*(6), 1049–1055. https://doi.org/10.1007/s00198-009-0854-9

[30] Zysset, P. K., Guo, X. E., Hoffler, C. E., Moore, K. E., & Goldstein, S. A. (1998). Mechanical properties of human trabecular bone lamellae quantified by nanoindentation. *Technology and Health Care: Official Journal of the European Society for Engineering and Medicine*, *6*(5–6), 429–432.

[31] Zysset, P. K., Guo, X. E., Hoffler, C. E., Moore, K. E., & Goldstein, S. A. (1999). Elastic modulus and hardness of cortical and trabecular bone lamellae measured by nanoindentation in the human femur. *Journal of Biomechanics*, *32*(10), 1005–1012. https://doi.org/10.1016/s0021-9290(99)00111-6